『岡山商大論叢』（岡山商科大学）
第42巻第3号　2007年3月
Journal of OKAYAMA SHOKA UNIVERSITY
Vol. 42　No. 3　March 2007

《論　　説》

Numerical Fourier transforms applied to Molière's series function and error analyses with the Takahasi-Mori theory of error evaluation

Takao Nakatsuka, Kazuhide Okei*, and Naoya Takahashi*

Abstract

Method of numerical Fourier transforms is applied to derive Molière's series functions for multiple Coulomb scattering. The results are compared with those derived by analytical method. Convergence of the numerical transforms is confirmed by applying Takahasi-Mori theory of error evaluation on the results.

1　Introduction

To solve diffusion equations in theoretical studies of particle transport, methods of functional transforms are effective. We can solve the equation comparatively easily by the method in the image space of transforms and we can derive the resultant probability density by applying inverse transforms to the solution. In the final stage of derivation we usually used analytical methods for particle transport

* Dept. of Natural Science, Okayama University.

problems, searching for exact analytical solutions in mathematical tables of the functional transforms or applying analytical approximation methods e.g. the saddle point method [1, 2] or others. If numerical methods for functional transforms were applicable, our knowledge of particle transport problems for fast charged particles and cascade shower particles would be increased. So we examine the reliability of numerical functional transforms applied to derive Molière's series functions [3, 4, 5] by comparing results with those derived by analytical methods.

Andreo, Medin, and Bielajew have already applied a numerical method of functional transforms on derivation of Molière's series function by using a tool in mathematical libraries [6]. It will be necessary and interesting to confirm reliability of numerical functional transforms by error analyses. We apply Takahasi-Mori theory of error evaluation based on the complex function theory [7] to investigate accuracy and efficiency of the method applied on the particle transport problems. Accuracy of our analytical result on Molière's series function of higher orders [8] will also be confirmed in these investigations. To examine efficiency of Takahasi-Mori theory in the particle transport problems will also be valuable for future applications in those problems.

2 Numerical Fourier transforms for Molière's series function

The spatial angular distribution and the projected angular distribution of fast charged particle traversing through material, $f(\vartheta)\vartheta d\vartheta$ and $f_{\mathrm{P}}(\varphi)d\varphi$, are expressed by Molière series expansion as

$$f(\vartheta) = f^{(0)}(\vartheta) + B^{-1}f^{(1)}(\vartheta) + B^{-2}f^{(2)}(\vartheta) + \ldots, \tag{1}$$

$$f_{\mathrm{P}}(\varphi) = f_{\mathrm{P}}^{(0)}(\varphi) + B^{-1}f_{\mathrm{P}}^{(1)}(\varphi) + B^{-2}f_{\mathrm{P}}^{(2)}(\varphi) + \ldots, \tag{2}$$

where the series functions $f^{(n)}(\vartheta)$ and $f_{\mathrm{P}}^{(n)}(\varphi)$ are expressed as

$$f^{(n)}(\vartheta) = \frac{1}{n!}\int_0^\infty y dy J_0(\vartheta y) e^{-\frac{y^2}{4}} \left(\frac{y^2}{4}\ln\frac{y^2}{4}\right)^n, \tag{3}$$

$$f_{\mathrm{P}}^{(n)}(\varphi) = \frac{2}{\pi n!}\int_0^\infty dy \cos(\varphi y) e^{-\frac{y^2}{4}} \left(\frac{y^2}{4}\ln\frac{y^2}{4}\right)^n. \tag{4}$$

We evaluate both the Molière series functions by numerical integration by trapezoidal method :

$$f^{(n)}(\vartheta) \simeq \frac{h}{n!}\sum_{k=0}^{\infty}{}' k J_0(\vartheta hk) e^{-\frac{h^2k^2}{4}} \left(\frac{h^2k^2}{4}\ln\frac{h^2k^2}{4}\right)^n, \tag{5}$$

$$f_{\mathrm{P}}^{(n)}(\varphi) \simeq \frac{2h}{\pi n!}\sum_{k=0}^{\infty}{}' \cos(\varphi hk) e^{-\frac{h^2k^2}{4}} \left(\frac{h^2k^2}{4}\ln\frac{h^2k^2}{4}\right)^n, \tag{6}$$

where $\sum'$ denotes the values should be taken half at the both ends of summation. The conditions of convergence are

1. The step size h of each summation is taken 10^{-4}.
2. The summation interval reaches up to where amplitudes of oscillating integrand do not exceed 10^{-20}.

We compared the results with those derived by analytical method [8] in Figs. 3–9 for spatial distributions and in Figs. 10–16 for projected distributions. The both results derived by numerical functional transforms and analytical method agree very well. And our results also agree very well with Andreo et al.'s derived using tools in mathematical library and their numerical integrations [6].

3 Error analyses of numerical integrations with Takahasi-Mori theory

Takahasi and Mori developed a new method to evaluate errors of numerical integration based on the complex function theory [7]. We can approximate a

definite integral

$$I \equiv \int_a^b f(x)dx \tag{7}$$

by a numerical integration

$$I_a \equiv \sum A_k f(a_k). \tag{8}$$

According to Takahasi and Mori, applying Cauchy integral theorem

$$f(x) = \frac{1}{2\pi i} \oint \frac{f(z)}{z-x} dz, \tag{9}$$

error of the numerical integration $\triangle I$ can be evaluated as

$$\begin{aligned}
\triangle I &\equiv I - I_a \\
&= \frac{1}{2\pi i} \oint \left(\int_a^b dx \frac{f(z)}{z-x} - \sum \frac{A_k}{z-a_k} f(z) \right) dz \\
&= \frac{1}{2\pi i} \oint \left(\ln \frac{z-a}{z-b} - \sum \frac{A_k}{z-a_k} \right) f(z) dz \\
&\equiv \frac{1}{2\pi i} \oint \Phi(z) f(z) dz,
\end{aligned} \tag{10}$$

where $\Phi(z)$ is called the characteristic function of error evaluation determined by the method of numerical integration irrespective of the integrand function.

In case of a numerical integration for infinite interval $(-\infty, \infty)$ by the trapezoidal method,

$$I = \int_0^\infty g(x)dx \simeq h \sum_{k=-\infty}^{\infty} g(hk). \tag{11}$$

Then the characteristic function $\Phi(z)$ is determined as

$$\Phi(z) = \lim_{k\to\infty} \ln\frac{z+kh}{z-kh} - \sum_{k=-\infty}^{\infty} \frac{h}{z-kh}$$

$$= \lim_{k\to\infty} \ln\left(-1-\frac{h}{kh}\right) + \frac{h}{z} - 2hz\sum_{k=0}^{\infty}\frac{1}{z^2-k^2h^2}$$

$$= -\pi\left\{i\,\mathrm{Sign}(\mathrm{Im}\,z) + \cot\frac{\pi z}{h}\right\}$$

$$\simeq \pm 2\pi i e^{\pm 2\pi i z/h}, \tag{12}$$

where the sign ± should agree with the sign of the imaginary component of z.

In case of a numerical integration for semi-infinite interval (0, ∞) by the trapezoidal method,

$$I = \int_0^{\infty} g(x)dx \simeq h\sum_{k=0}^{\infty} g(hk). \tag{13}$$

Then the characteristic function $\Phi(z)$ is determined as

$$\Phi(z) = \ln\left(-\frac{z}{h}\right) + \frac{h}{2z} - \psi\left(-\frac{z}{h}\right)$$

$$= \ln\left(-\frac{z}{h}\right) - \frac{h}{2x} - \psi\left(\frac{z}{h}\right) - \pi\cot\frac{\pi z}{h}. \tag{14}$$

As it approximately satisfies

$$\psi(z) \simeq \ln z - \frac{1}{2z}, \tag{15}$$

$\Phi(z)$ can be well approximated as

$$\Phi(z) \simeq -\pi\left(i\,\mathrm{Sign}(\mathrm{Im}\,z) + \cot\frac{\pi z}{h}\right), \tag{16}$$

by that for infinite interval [7].

4 Error analyses of Molière series function for projected angular distribution

The integral (4) for semi-infinite interval can be evaluated by the integral for infinite interval with the integrand extended on the negative real axis, as the integrand is even. So we can evaluate the error of (4) by the formula for infinite interval, thus the error can be evaluated as

$$\triangle I_{\mathrm{P}}^{(n)} = \frac{1}{2\pi i}\oint \Phi(z)g(z)dz, \quad \text{where} \tag{17}$$

$$g(z) = \frac{1}{\pi n!}\cos(\varphi z)e^{-\frac{z^2}{4}}\left(\frac{z^2}{4}\ln\frac{z^2}{4}\right)^n, \tag{18}$$

with $\Phi(z)$ of Eq. (12). The path of complex integration is a pair of parallel straight lines, from $iy_0 + i\infty$ to $iy_0 - i\infty$ with y_0 positive and from $iy_0 - i\infty$ to $iy_0 + i\infty$ with y_0 negative.

For $n = 0$,

$$\triangle I_{\mathrm{P}}^{(n)} = \frac{1}{\pi}\frac{1}{2\pi i}\oint \Phi(z)\cos(\phi z)e^{-\frac{z^2}{4}}dz. \tag{19}$$

This integral can be well evaluated by the saddle point method [1, 2] :

$$\triangle I_{\mathrm{P}}^{(n)} \simeq -\frac{2}{\sqrt{\pi}}e^{-{y_0}^2/4}, \tag{20}$$

where the saddle points exist at

$$\overline{z} = \pm y_0 i, \quad \text{where} \quad \frac{y_0}{2} \equiv \frac{2\pi}{h} - \varphi. \tag{21}$$

For $n \geq 1$, the integrand $g(z)$ has a branch point at the origin. So we take account a schnitt between the origin and the saddle point $\overline{z} = y_0 i$ defined above and take the path as shown in Fig. 1. The contribution to $\triangle I_{\mathrm{P}}^{(n)}$ from the saddle points is about $\left(2/\sqrt{\pi}\right)e^{-{y_0}^2/4}$ and is negligible. The value of $\triangle I_{\mathrm{P}}^{(n)}$ is determined from the curvilinear integral at both sides of the schnitt :

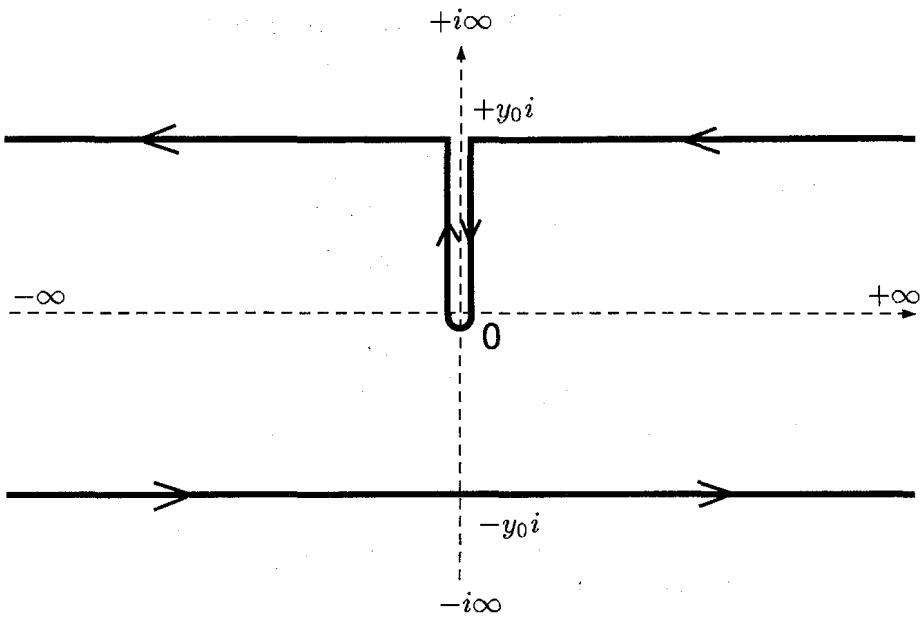

Figure 1 : Path of complex integral for $\triangle I_{\mathrm{P}}^{(n)}$ with $n \geq 1$.

$$\triangle I_{\mathrm{P}}^{(n)} = \frac{-1}{2\pi i}\int_0^{y_0} \pi i \frac{e^{-\pi y/h}}{\sinh(\pi y/h)} \frac{1}{\pi n!} \cosh(\varphi y)\, e^{\frac{y^2}{4}} \left(-\frac{y^2}{4}\right)^n$$

$$\left\{\left(\ln\frac{y^2}{4} + 4\pi i\right)^n - \left(\ln\frac{y^2}{4}\right)^n\right\} i dy. \tag{22}$$

For enough small step size of numerical integration the factor $e^{y^2/4}\cosh(\varphi y)$ can be neglected as they satisfy $\pi/h \gg \varphi$ and $\pi/h \gg 1$, so we have

$$\triangle I_{\mathrm{P}}^{(n)} \simeq \frac{2(-1)^n}{(n-1)!}\int_0^{y_0} \left(\frac{y^2}{4}\right)^n \left(\ln\frac{y^2}{4}\right)^{n-1} \frac{e^{-\pi y/h}}{\sinh(\pi y/h)} dy$$

$$\simeq \frac{2(-1)^n}{(n-1)!}\left[\frac{d^{n-1}}{dp^{n-1}}\int_0^{\infty} \left(\frac{y^2}{4}\right)^p \frac{e^{-\pi y/h}}{\sinh(\pi y/h)} dy\right]_{p=n}$$

$$= \frac{2(-1)^n}{(n-1)!}\frac{d^{n-1}}{dp^{n-1}}\left[2\left(\frac{2\pi}{h}\right)^{-2p-1}\int_0^{\infty} t^{2p}\frac{e^{-t}}{\sinh t} dt\right]_{p=n}$$

$$\simeq \frac{-4}{(n-1)!}\left(2\ln\frac{2\pi}{h}\right)^{n-1}\left(\frac{2\pi}{h}\right)^{-2n-1}\int_0^{\infty} t^{2n}\frac{e^{-t}}{\sinh t} dt$$

Table 1 : Values of ζ-function.

n	$\zeta(n)$
3	1.20206
5	1.03693
7	1.00835
9	1.00201
11	1.00049
13	1.00012

$$= -2n(2n-1)!!\zeta(2n+1)\left(\ln\frac{2\pi}{h}\right)^{n-1}\left(\frac{2\pi}{h}\right)^{-2n-1}, \qquad (23)$$

where $\zeta(k)$ denotes ζ-function [9], as indicated in Table 1. The results of $\triangle I_P^{(n)}$ are indicated in Figs. 17–23 for n of 0 to 6.

5 Error analyses of Molière series function for spatial angular distribution

Molière series function for spatial angular distribution (3) is derived from the integral over semi-infinite interval (0, ∞). The error of numerical integration (5) can be evaluated by the complex integral (10) of Takahasi-Mori theory :

$$\triangle I^{(n)} = \frac{1}{2\pi i}\oint \Phi(z)g(z)dz, \quad \text{where} \qquad (24)$$

$$g(z) = \frac{1}{n!}zJ_0(\vartheta z)e^{-\frac{z^2}{4}}\left(\frac{z^2}{4}\ln\frac{z^2}{4}\right)^n, \qquad (25)$$

with the approximated characteristic function $\Phi(z)$ of Eq. (12) [7]. The path of complex integration is taken as a straight line parallel to the real axis with positive imaginary component y_0 and real component from ∞ to 0, a straight line on the imaginary axis from iy_0 to $-iy_0$, and a straight line parallel to the real axis with negative imaginary component $-y_0$ and real component from 0 to ∞, as shown in Fig. 2.

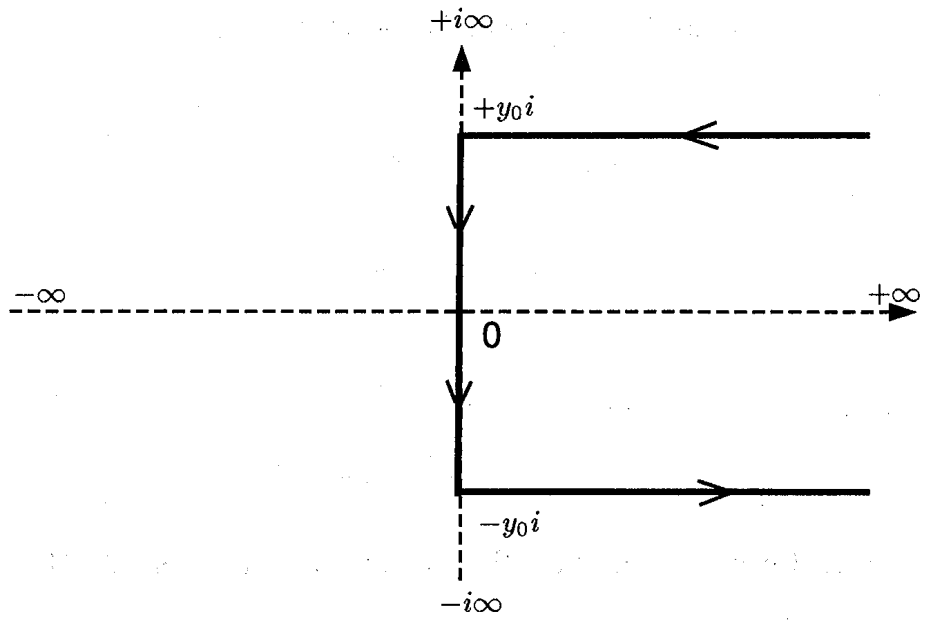

Figure 2 : Path of complex integral for $\triangle I^{(n)}$.

Taking account $g(z)$ is odd and $\Phi(z)$ falls extremely rapidly at positions far from the real axis, $\triangle I^{(n)}$ can be evaluated as

$$\triangle I^{(n)} = \frac{1}{2\pi i}\int_{y_0 i}^{-y_0 i} \frac{\Phi(z)}{2}\frac{1}{n!} z J_0(\vartheta z)\exp\left(-\frac{z^2}{4}\right)\left(\frac{z^2}{4}\ln\frac{z^2}{4}\right)^n dz$$

$$= \frac{-1}{2\pi i}\frac{1}{n!}\int_0^{y_0} \pi i \frac{e^{-\pi y/h}}{\sinh(\pi y/h)}\left(\frac{-y^2}{4}\right)^n$$

$$\frac{1}{2}\left\{\left(\ln\frac{y^2}{4}+\pi i\right)^n + \left(\ln\frac{y^2}{4}-\pi i\right)^n\right\} iyidy$$

$$\simeq \frac{(-1)^n}{2n!}\left[\frac{d^n}{dp^n}\int_0^{\infty}\left(\frac{y^2}{4}\right)^p \frac{e^{-\pi y/h}}{\sinh(\pi y/h)} y dy\right]_{p=n}$$

$$= \frac{2(-1)^n}{n!}\left[\frac{d^n}{dp^n}\left\{\left(\frac{2\pi}{h}\right)^{-2p-2}\int_0^{\infty} t^{2p+1}\frac{e^{-t}}{\sinh t}dt\right\}\right]_{P=n}$$

$$\simeq \frac{2(n+1)}{n!}\left(\ln\frac{2\pi}{h}\right)^n\left(\frac{2\pi}{h}\right)^{-2n-2}\int_0^{\infty} t^{2n+1}\frac{e^{-t}}{\sinh t}dt$$

$$\simeq \frac{1}{n!}|B_{2n+2}|\left(\ln\frac{2\pi}{h}\right)^n\left(\frac{2}{h}\right)^{-2n-2}, \qquad (26)$$

Table 2 : Values of Bernoulli number.

n	B_n
2	1/6
4	−1/30
6	1/42
8	−1/30
10	5/66
12	−691/2730
14	7/6

where B_n denotes Bernoulli number [9], as indicated in Table 2. The results of $\triangle I^{(n)}$ are indicated in Figs. 24–30 for n of 0 to 6.

6 Conclusions and discussions

We have evaluated Molière series functions by numerical functional transforms up to 6-th higher terms for both spatial and projected angular distributions. The results have agreed very well with those derived by analytical method [8]. The results also have agreed very well with Andreo et al.'s given for spatial angular distributions [6].

Convergences of our numerical functional transforms are confirmed by error analyses of numerical integration developed by Takahasi and Mori [7]. Numerical transforms for the first term for projected angular distribution has converged as negative exponential with the division rate (division number per unit length) and those for other projected distributions and for spatial distributions have converged as negative power of respective index with the division rate, all satisfying Takahasi-Mori predictions.

These results will prove reliability of numerical functional transforms applied in particle transport problems, as well as efficiencies of Takahasi-Mori theory in these problems.

Aknowledgments

The authors wish to express their deep gratitude to Prof. Jun Nishimura for valuable advices and continuous encouragements.

References

[1] J. Nishimura, in *Handbuch der Physik, Band 46*, edited by S. Flügge (Springer, Berlin, 1967), Teil **2**, p. 1.
[2] T. Nakatsuka, Phys. Rev. **D35**, 210 (1987).
[3] G. Molière, Z. Naturforsch. **2a**, 133 (1947).
[4] G. Molière, Z. Naturforsch. **3a**, 78 (1948).
[5] H.A. Bethe, Phys. Rev. **89**, 1256 (1953).
[6] P. Andreo, J. Medin, and A. F. Bielajew, Med. Phys. **20**, 1315 (1993).
[7] H. Takahasi and M. Mori, Rep. Compt. Centre, Univ. Tokyo, **3**, 41 (1970).
[8] T. Nakatsuka, Journal of Okayama Shoka University, **42**, No. 2, 1 (2006).
[9] *Handbook of Mathematical Functions with Formulas, Graphs, and Mathematical Tables*, edited by M. Abramowitz and I. A. Stegun (Dover, New York, 1965).

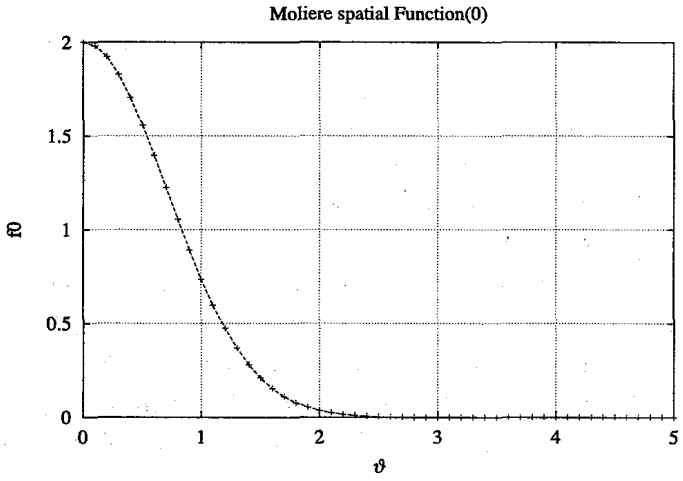

Figure 3 : Comparison of Molière series function for spatial angular distribution, $f^{(0)}(\vartheta)$, derived by the numerical method (dots) and the analytical method (lines).

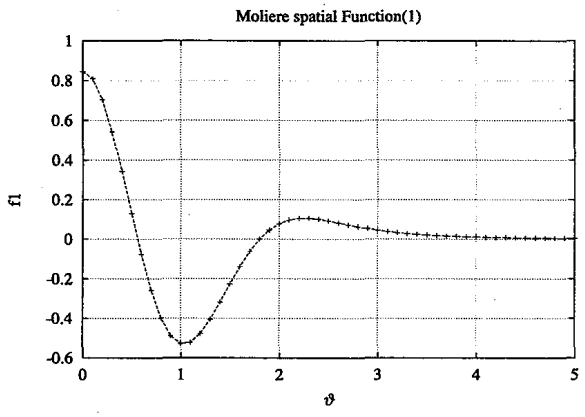

Figure 4 : Comparison of $f^{(1)}(\vartheta)$.

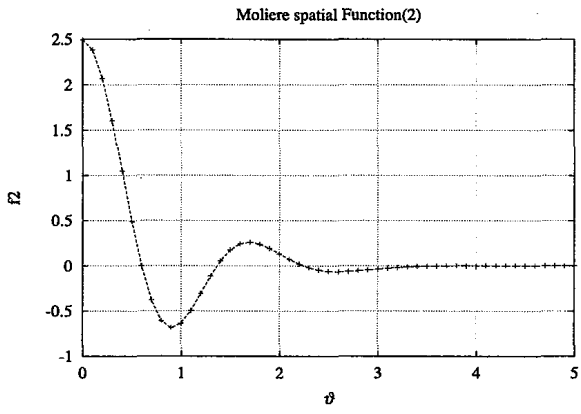

Figure 5 : Comparison of $f^{(2)}(\vartheta)$.

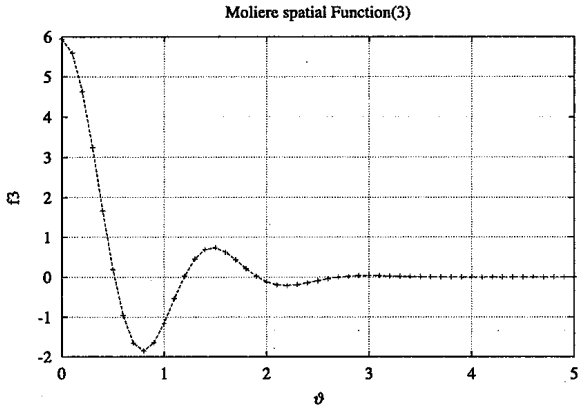

Figure 6 : Comparison of $f^{(3)}(\vartheta)$.

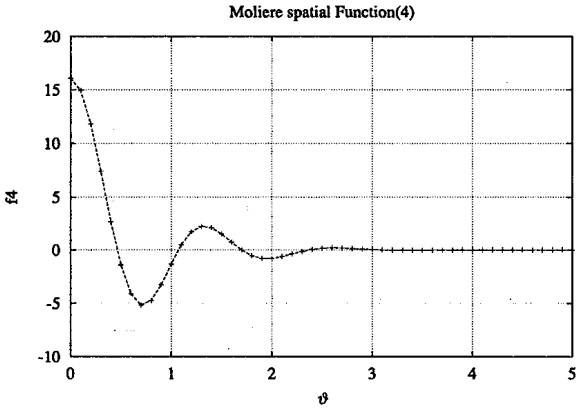

Figure 7 : Comparison of $f^{(4)}(\vartheta)$.

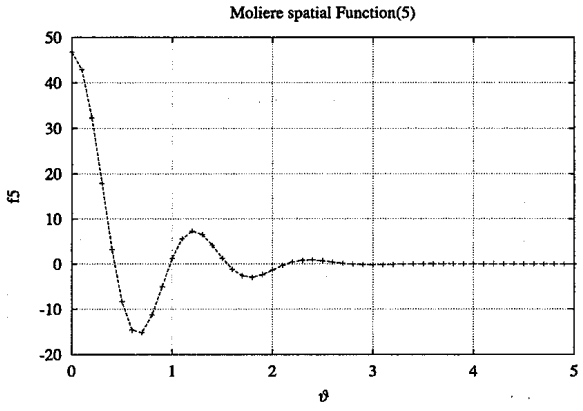

Figure 8 : Comparison of $f^{(5)}(\vartheta)$.

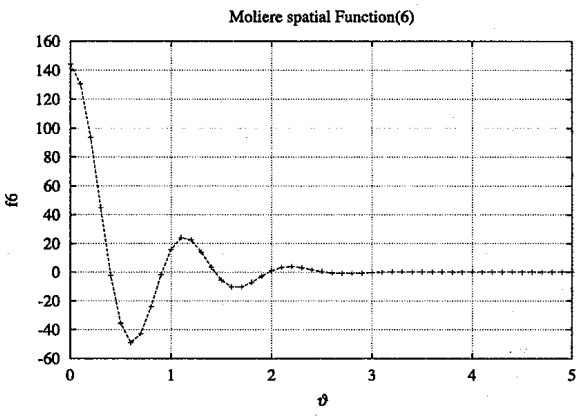

Figure 9 : Comparison of $f^{(6)}(\vartheta)$.

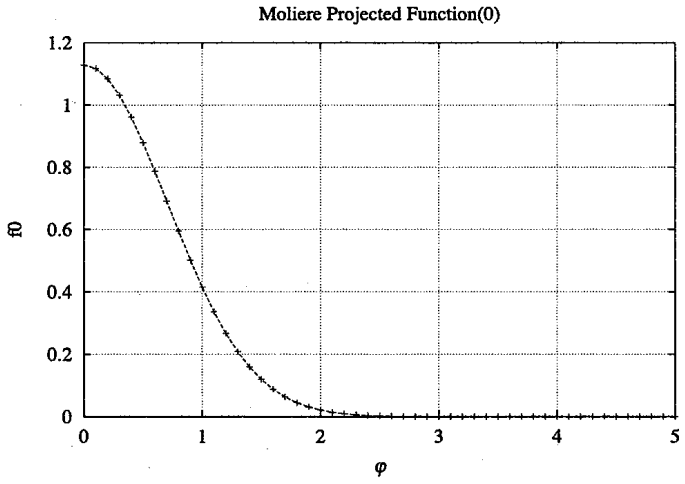

Figure 10 : Comparison of Molière series function for projected angular distribution, $f_P^{(0)}(\varphi)$, derived by the numerical method (dots) and the analytical method (lines).

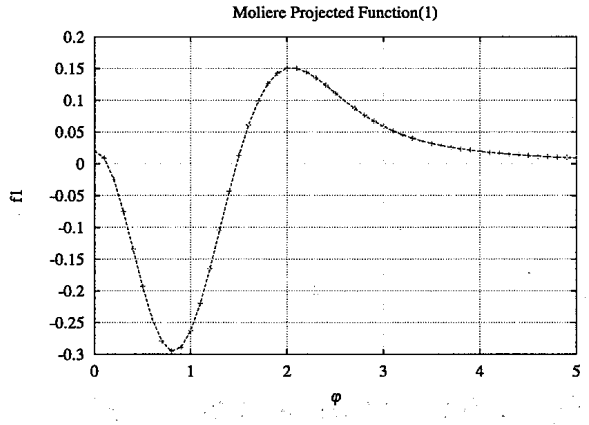

Figure 11 : Comparison of $f_P^{(1)}(\varphi)$.

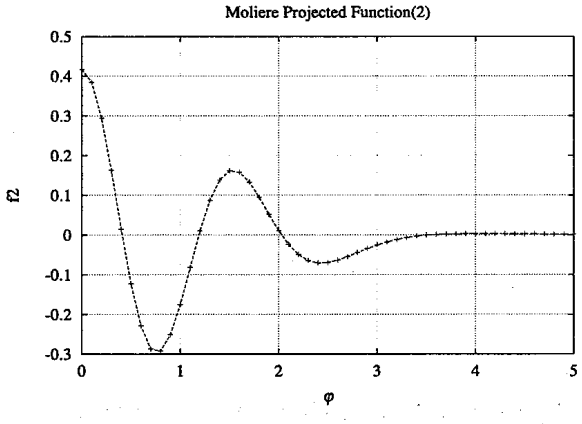

Figure 12 : Comparison of $f_P^{(2)}(\varphi)$.

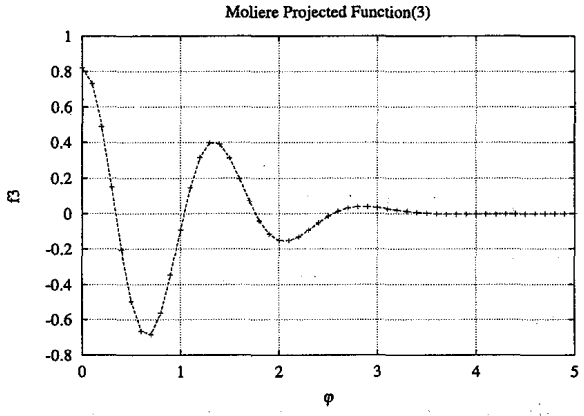

Figure 13 : Comparison of $f_{\mathrm{P}}^{(3)}(\varphi)$.

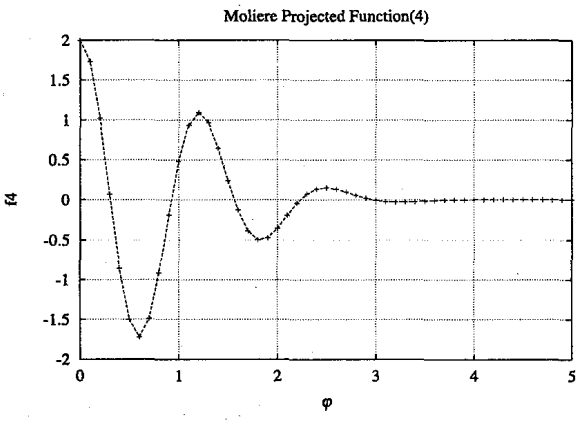

Figure 14 : Comparison of $f_{\mathrm{P}}^{(4)}(\varphi)$.

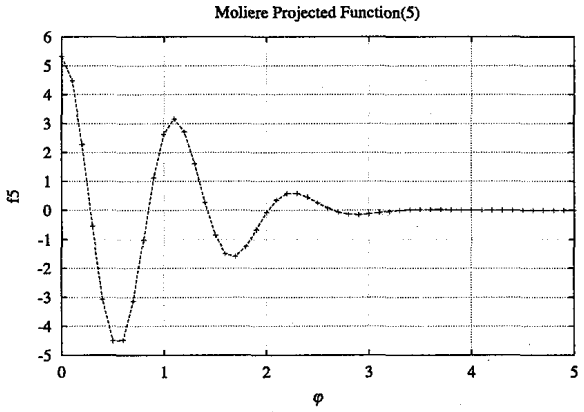

Figure 15 : Comparison of $f_{\mathrm{P}}^{(5)}(\varphi)$.

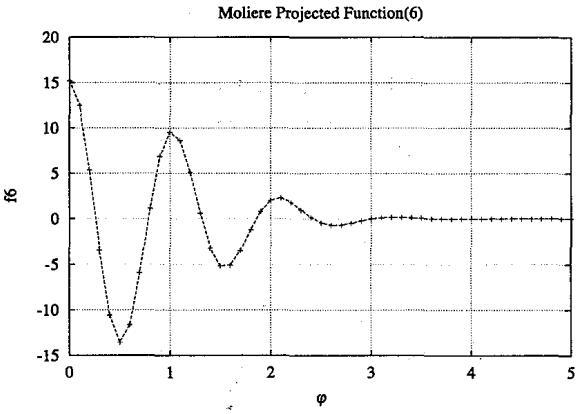

Figure 16 : Comparison of $f_{\mathrm{P}}^{(6)}(\varphi)$.

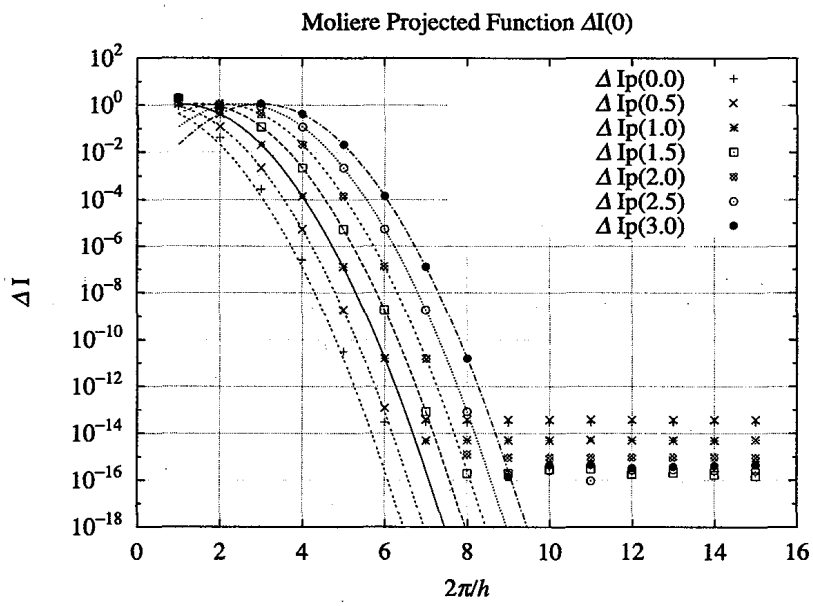

Figure 17: Error evaluation, $\triangle I_{\mathrm{P}}^{(0)}$, vs the division rate in derivation of Molière series function for projected angular distribution. Our calculations (dots) agree well with Takahasi-Mori predictions (lines).

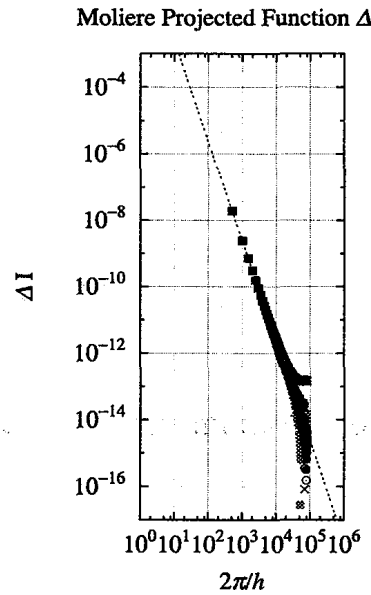

Figure 18 : Evaluation $\triangle I_{\mathrm{P}}^{(1)}$.

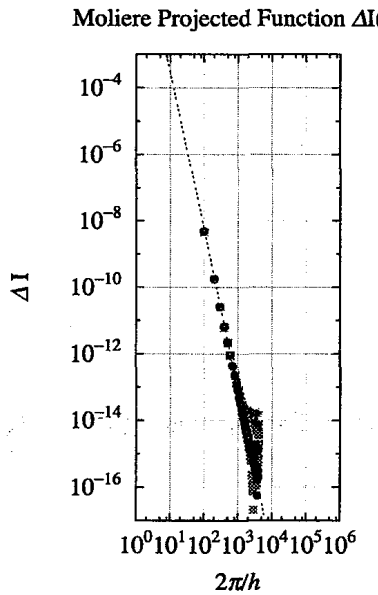

Figure 19 : Evaluation $\triangle I_{\mathrm{P}}^{(2)}$.

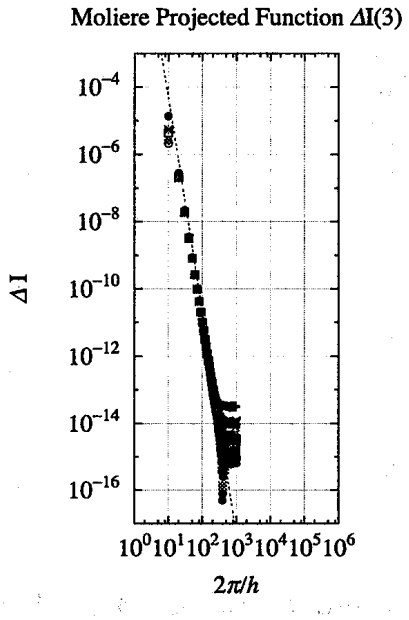

Figure 20 : Evaluation $\triangle I_{\mathrm{P}}^{(3)}$.

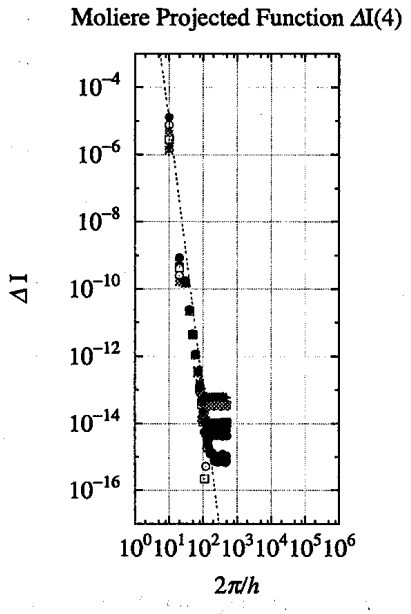

Figure 21 : Evaluation $\triangle I_{\mathrm{P}}^{(4)}$.

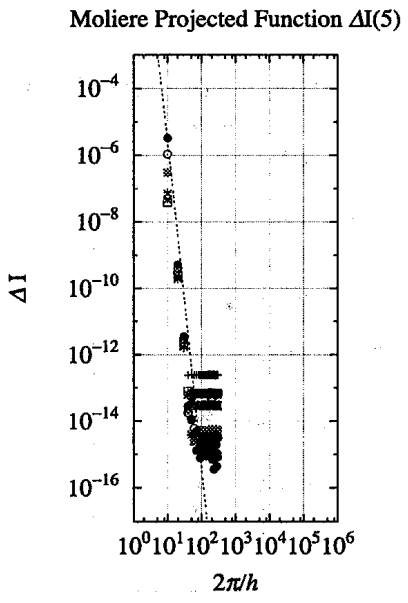

Figure 22 : Evaluation $\triangle I_{\mathrm{P}}^{(5)}$.

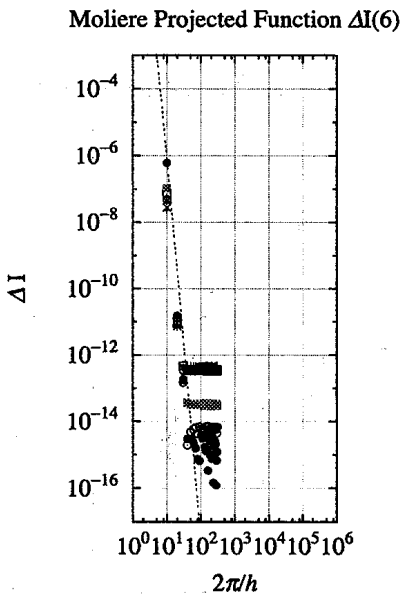

Figure 23 : Evaluation $\triangle I_{\mathrm{P}}^{(6)}$.

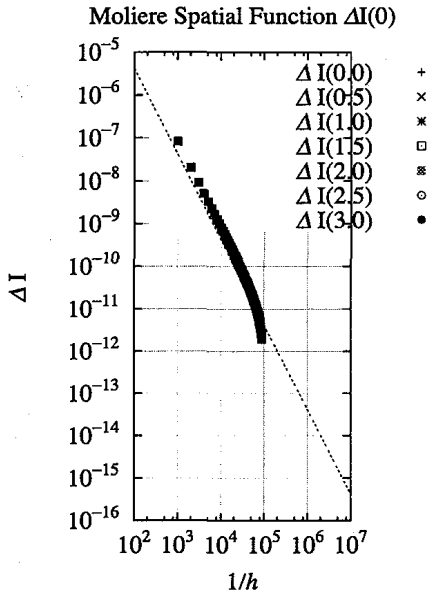

Figure 24: Error evaluation, $\triangle I^{(0)}$, vs the division rate in derivation of Molière series function for spatial angular distribution. Our calculations (dots) agree well with Takahasi-Mori predictions (lines).

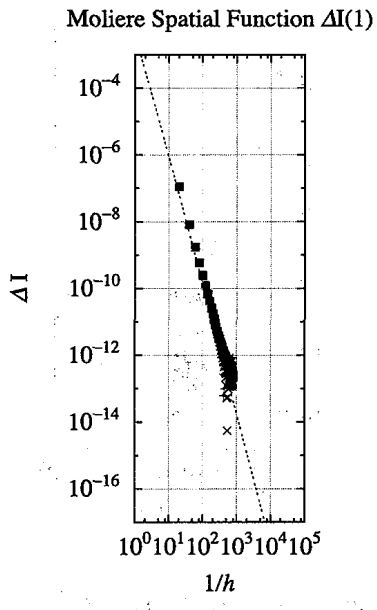

Figure 25 : Evaluation $\triangle I^{(1)}$.

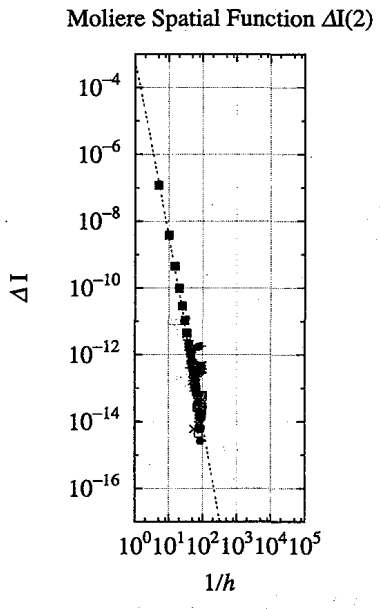

Figure 26 : Evaluation $\triangle I^{(2)}$.

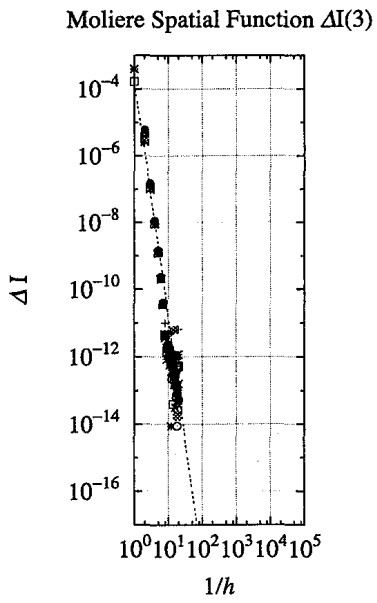

Figure 27 : Evaluation $\triangle I^{(3)}$.

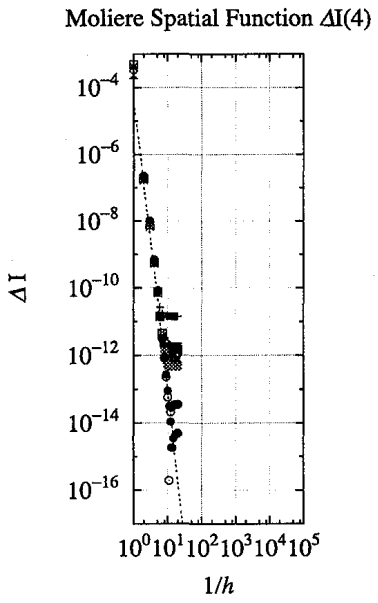

Figure 28 : Evaluation $\triangle I^{(4)}$.

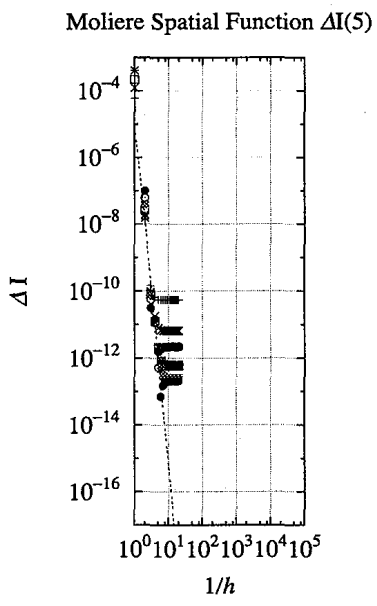

Figure 29 : Evaluation $\triangle I^{(5)}$.

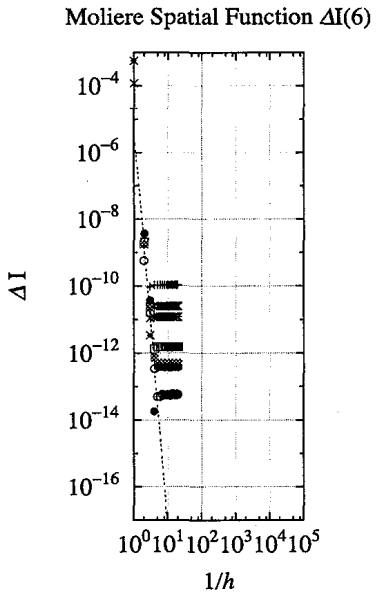

Figure 30 : Evaluation $\triangle I^{(6)}$.